Theory of 2D Transport in Graphene for Correlated Disorder

Qiuzi Li,[1] E. H. Hwang,[1] E. Rossi,[2] and S. Das Sarma[1]

[1]*Condensed Matter Theory Center, Department of Physics, University of Maryland, College Park, Maryland 20742, USA*
[2]*Department of Physics, College of William and Mary, Williamsburg, Virginia 23187, USA*

(Received 22 June 2011; published 5 October 2011)

We theoretically revisit graphene transport properties as a function of carrier density, taking into account possible correlations in the spatial distribution of the Coulomb impurity disorder in the environment. We find that the charged impurity correlations give rise to a density-dependent graphene conductivity, which agrees well qualitatively with the existing experimental data. We also find, quite unexpectedly, that the conductivity could increase with increasing impurity density if there is sufficient interimpurity correlation present in the system. In particular, the linearity (sublinearity) of graphene conductivity at lower (higher) gate voltage is naturally explained as arising solely from impurity correlation effects in the Coulomb disorder.

DOI: 10.1103/PhysRevLett.107.156601 PACS numbers: 72.80.Vp, 81.05.ue, 72.10.−d, 73.22.Pr

One of the most studied properties of graphene is its electrical conductivity as a function of the applied gate voltage which translates directly into the carrier density-(n-) dependent conductivity $\sigma(n)$ [1]. The functional dependence of $\sigma(n)$ at low temperatures contains information [1] about the nature of disorder in the graphene environment giving rise to the dominant resistive carrier scattering mechanism. Although there is a well-accepted theory [1] for graphene transport involving an interplay between long-range charged impurity and short-range disorder scattering, the theory is not universally accepted and cannot explain all experimental observations, indicating the possibility of important missing ingredients [2].

In this work, we provide a qualitatively new theory for the $\sigma(n)$ properties of graphene and introduce a new physical explanation for the experimental observations; i.e., we explain why $\sigma(n) \sim n$ for "small" or "intermediate" n and $\sigma(n) \sim$ const for "large" n, with a smooth nonlinear crossover between the two asymptotic behaviors. We also provide theoretical results for $\sigma_{\min}$, the graphene minimum conductivity at the Dirac point, using our new theory. We concentrate on the nature of the underlying static disorder limiting graphene transport in currently available samples where phonon scattering effects are relatively weak (compared with disorder scattering) even at room temperature [3]. The quantitative weakness of the electron-phonon interaction in graphene gives particular impetus to a thorough understanding of the disorder mechanisms limiting graphene conductivity, since this may enable substantial enhancement of room temperature graphene-based device speed for technological applications as disorder remains the primary resistive mechanism limiting graphene transport even at room temperature. Therefore, a complete understanding of the disorder mechanisms controlling $\sigma(n)$ in graphene at $T = 0$ is of utmost importance from both fundamental and technological perspectives.

The most important features of the experimentally observed $\sigma(n)$ [4–8] in graphene are (i) a nonuniversal sample-dependent minimum conductivity $\sigma(n \approx 0) \equiv \sigma_{\min}$ at the charge neutrality point (CNP) where the average carrier density vanishes, (ii) a linearly increasing, $\sigma(n) \propto n$, conductivity with increasing carrier density on both sides of the CNP up to some sample-dependent characteristic carrier density, and (iii) a sublinear $\sigma(n)$ for high carrier density, making it appear that the very high-density $\sigma(n)$ may be saturating.

A successful model [1,9–12] for diffusive graphene carrier transport incorporates two distinct scattering mechanisms with individual resistivity ρ_c and ρ_s, arising, respectively, from the long-range Coulomb disorder due to random background charged impurities and static zero-range (often called "short-range") disorder. The net graphene conductivity is then given by $\sigma \equiv \rho^{-1} = (\rho_c + \rho_s)^{-1}$. It is easy to show that [1,9–12] $\rho_c \sim 1/n$ and $\rho_s \sim$ const in graphene, leading to $\sigma(n)$ going as $\sigma(n) = n/(A + Cn)$, where the constants A and C are known [1] as functions of disorder parameters; A, arising from Coulomb disorder, depends on the impurity density (n_i) (and also on their locations in space) and the background dielectric constant (κ), whereas the constant C, arising from the short-range disorder [1,11], depends on the strength of the white-noise disorder characterizing the zero-range scattering. The relation $\sigma(n) = n/(A + Cn)$ explains the observed $\sigma(n)$ behavior of graphene for $n \neq 0$ since $\sigma(n \ll A/C) \sim n$, and $\sigma(n \gg A/C) \sim 1/C$ with $\sigma(n)$ showing sublinear $(C + A/n)^{-1}$ behavior for $n \sim A/C$.

The above-discussed scenario for disorder-limited graphene conductivity, with both long-range and short-range disorder playing important qualitative roles at intermediate ($n_i \lesssim n \lesssim A/C$) and high ($n > A/C$) carrier densities respectively, has been experimentally verified by several groups [5–8]. There is, however, one *serious issue* with

this reasonable scenario: Although the physical mechanism underlying the long-range disorder scattering is experimentally established [1,5,6] to be the presence of unintentional charged impurity centers in the graphene environment, the physical origin of the short-range disorder scattering is unclear and experimentally obscure. Point defects (e.g., vacancies) are rare in graphene, producing negligible short-range disorder. There have also been occasional puzzling conductivity measurements (e.g., Ref. [13]) reported in the literature which do not appear to be easily explicable by using the standard model of independent dual scattering by long- and short-range disorder playing equivalent roles.

In this Letter, we propose an alternative physical model for understanding disorder-limited $\sigma(n)$ behavior in graphene. The model is simpler (and, therefore, more appealing) than the standard model of independent dual disorder mechanisms, because it requires only the long-range Coulomb disorder associated with the background charged impurities eliminating completely the *ad hoc* short-range disorder necessary for explaining the high-density nonlinearity in $\sigma(n)$. Our model, therefore, eliminates the undesirable feature of the standard model; namely, no adjustable short-range scattering term with unknown physical origin needs to be arbitrarily added to the problem in order to explain the observed high-density sublinear $\sigma(n)$.

The key to our model is the inclusion of some *spatial correlations* in the distribution of the charged impurity locations in the system; i.e., the charged impurities are no longer considered to be completely random spatially. Some impurity correlations are perfectly reasonable to assume, since much of the fabrication and processing of graphene is done at room temperature (and, in fact, often thermal and/or current annealing is used in sample preparation), which is expected to lead to actual diffusion of the impurities producing an annealed, at least partially, correlated impurity configuration rather than a quenched uncorrelated random one. We show that the single assumption of impurity correlations, defined through a correlation length scale parameter r_0, is sufficient to explain the qualitative features of the experimental $\sigma(n)$ behavior by using only disorder scattering by background charged impurities.

To calculate the impurity correlations, we use Monte Carlo simulations carried out on a 200×200 triangular lattice with 10^6 averaging runs, periodic boundary conditions, and a lattice constant $a_0 = 4.92$ Å, which is 2 times the graphene lattice constant, since the most closely packed phase of impurity atoms (e.g., K as in Ref. [6]) on graphene is likely to be an $m \times m$ phase with $m = 2$ for K [14]. Correlations are automatically introduced by virtue of the random positioning of the impurities at lattice sites with the correlation length $r_0 < r_i = (\pi n_i)^{-1/2}$. Our correlation model is physically motivated with the reasonable underlying assumption that two impurities cannot be arbitrarily close to each other (as they can be in the unphysical continuum random impurity model, where $r_0 = 0$), and there must be a minimum separation between them. A reasonable continuum approximation to this discrete lattice model is given by the following pair distribution function $g(\mathbf{r})$ ($\mathbf{r}$ is a 2D vector in the graphene plane):

$$g(\mathbf{r}) = \begin{cases} 0 & |\mathbf{r}| \le r_0 \\ 1 & |\mathbf{r}| > r_0 \end{cases} \tag{1}$$

for the impurity density distribution. Even though Eq. (1) is only an approximation, the basic idea of a length scale r_0 defining the spatial impurity correlations is physically sound (with $r_0 = 0$ for the purely random case). Impurity correlation effects enter the transport theory through the structure factor $S(\mathbf{q})$, given by $S(\mathbf{q}) = 1 + n_i \int d^2 r e^{i\mathbf{q}\cdot\mathbf{r}}[g(\mathbf{r}) - 1]$. For uncorrelated random impurity scattering, as in the standard theory, $g(\mathbf{r}) = 1$ always, and $S(\mathbf{q}) \equiv 1$. With Eq. (1), we have

$$S(q) = 1 - 2\pi n_i \frac{r_0}{q} J_1(q r_0), \tag{2}$$

where $J_1(x)$ is the Bessel function of the first kind. Figure 1(a) shows the structure factor $S(\mathbf{q})$ obtained from the Monte Carlo simulations. Figure 1(b) shows $S(\mathbf{q})$ for both the random Monte Carlo realistic numerical model and the simple continuum analytic approximation [Eq. (2)]. It is obvious that the analytic approximation captures well the essential features of the full numerical Monte Carlo simulation.

The graphene carrier conductivity due to scattering by screened Coulomb disorder can now be calculated by taking into account the impurity correlations, leading to $\sigma = (e^2/h)(g E_F \tau)/(2\hbar)$, where E_F is the Fermi energy, $g = 4$ is the total degeneracy of graphene, and the transport relaxation time τ is given by [15]

$$\frac{\hbar}{\tau} = \left(\frac{\pi n_i \hbar v_F}{4 k_F}\right) r_s^2 \int \frac{d\theta (1 - \cos^2\theta)}{(\sin\frac{\theta}{2} + 2 r_s)^2} S\left(2 k_F \sin\frac{\theta}{2}\right), \tag{3}$$

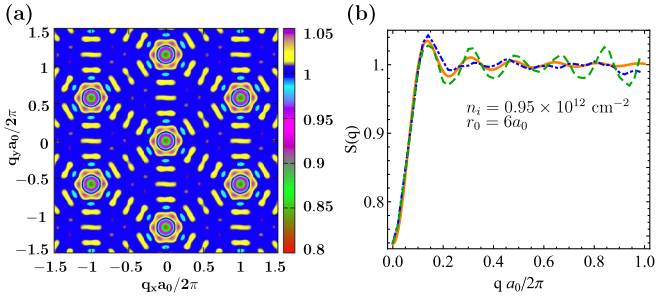

FIG. 1 (color online). (a) Density plot of structure factor $S(\mathbf{q})$ obtained from Monte Carlo simulations for $n_i = 0.95 \times 10^{12}$ cm^{-2}, $a_0 = 4.92$ Å, and $r_0 = 5a_0$. (b) Structure factor $S(\mathbf{q})$ using Eq. (2) (solid line) and Monte Carlo simulations. Dot-dashed and dashed lines show the Monte Carlo results for two different directions of $\mathbf{q}$ from the x axis: $\theta = 0$ and $\theta = 30°$, respectively.

where v_F is the graphene Fermi velocity, k_F the Fermi wave vector [$k_F = E_F/(\hbar v_F)$], and r_s the graphene fine structure constant [$r_s = e^2/(\hbar v_F \kappa)$]. For uncorrelated random impurity scattering, $r_0 = 0$, $g(\mathbf{r}) = 1$, and $S(\mathbf{q}) \equiv 1$, we recover the standard formula for Boltzmann conductivity by screened random charged impurity centers [11,12]. In addition to scattering, charge impurities induce strong carrier density inhomogeneities in graphene, especially close to the CNP, that must be taken into account in the transport theory. To characterize these inhomogeneities we use the Thomas-Fermi-Dirac theory [16], assuming that the impurities are placed in a 2D plane at a distance $d = 1$ nm from the graphene layer. Figures 2(a) and 2(b) show the carrier density profile for a single disorder realization for the uncorrelated case and the correlated case ($r_0 = 10a_0$) for $n_i = 0.95 \times 10^{12}$ cm^{-2}. We can see that in the correlated case the amplitude of the density fluctuations is much smaller than in the uncorrelated case. The Thomas-Fermi-Dirac approach is very efficient and allows the calculation of disorder averaged quantities such as the density root mean square n_{rms} and the density probability distribution $P(n)$. Figures 2(c)–2(e) show $P(n)$ at the CNP and away from the Dirac point ($n_i = 0.95 \times 10^{12}$ cm^{-2}). In each figure, both the results for the uncorrelated case and the ones for the correlated case are shown. $P(n)$ for the correlated case is, in general, overall narrower than $P(n)$ for the correlated case, resulting in smaller values of n_{rms} as shown in Fig. 2(f), in which n_{rms}/n_i as a function of r_0/r_i is plotted for different values of the average density $\langle n \rangle$ and two different values of the impurity density: $n_i = 0.95 \times 10^{12}$ cm^{-2} ("low impurity density") for the solid lines and $n_i = 4.8 \times 10^{12}$ cm^{-2} ("high impurity density") for the dashed lines.

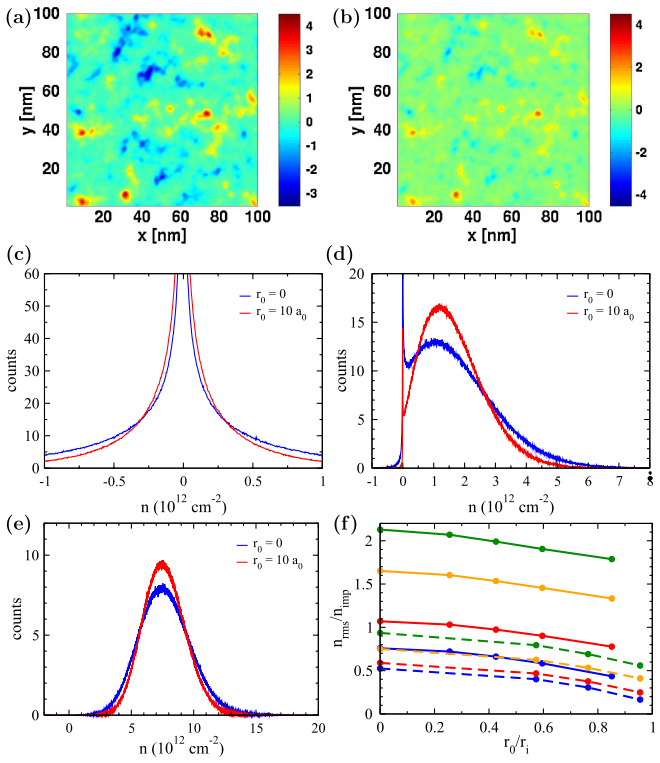

FIG. 2 (color online). The carrier density for a single disorder realization obtained from the Thomas-Fermi-Dirac theory (a) for the uncorrelated case and (b) $r_0 = 10a_0$ with $n_i = 0.95 \times 10^{12}$ cm^{-2}. Carrier probability distribution function $P(n)$ is shown in (c), (d), and (e) for $\langle n \rangle = 0$, 1.78, and 7.7×10^{12} cm^{-2}, respectively. In (f) the ratio n_{rms}/n_i is shown as a function of r_0/r_i for $n_i = 0.95 \times 10^{12}$ cm^{-2} (solid lines) and $n_i = 4.8 \times 10^{12}$ cm^{-2} (dashed lines). We use $\langle n \rangle = 7.7$, 3.14, 0.94, and 0×10^{12} cm^{-2} for the solid lines (from top to bottom) and $\langle n \rangle = 8.34$, 4.10, 1.7, and 0×10^{12} cm^{-2} for the dashed lines.

We now present our results for the conductivity. The integral in Eq. (3) can be calculated analytically for "small" k_F by expanding $S(x)$ in the integrand giving

$$\sigma(n) = An[1 - a + Ba^2 n/n_i]^{-1}, \tag{4}$$

where $A = \frac{e^2}{h}[2n_i r_s^2 G_1(r_s)]^{-1}$, $a = \pi n_i r_0^2$, and $B = G_2(r_s)/[2G_1(r_s)]$. Note that $a < 1$ in our model. The dimensionless functions $G_{1,2}(r_s)$ are given by $G_1(x) = \frac{\pi}{4} + 6x - 6\pi x^2 + 4x(6x^2 - 1)g(x)$ and $G_2(x) = \frac{\pi}{16} - \frac{4x}{3} + 3\pi x^2 + 40x^3[1 - \pi x + \frac{4}{5}(5x^2 - 1)g(x)]$, where $g(x) = \mathrm{sech}^{-1}(2x)/\sqrt{1 - 4x^2}$ for $x < \frac{1}{2}$ and $\sec^{-1}(2x)/\sqrt{4x^2 - 1}$ for $x > \frac{1}{2}$. Equation (4) indicates that, for small n, $\sigma(n) \sim An(1 - a)^{-1}$ and, for large n, $\sigma(n) \sim (1 - n_c/n)$, where $n_c = (1 - a)n_i/(Ba^2) \sim O(1/n_i r_0^4)$. The crossover density n_c, where the sublinearity ($n > n_c$) manifests itself, increases strongly with decreasing r_0. This generally implies that the higher mobility annealed samples should manifest stronger nonlinearity in $\sigma(n)$, since annealing leads to stronger impurity correlations (and hence larger r_0). This is exactly the experimental observation. While the resistivity within the standard random model increases linearly in n_i, Eq. (4) indicates that the resistivity could decrease with increasing impurity density if there are sufficient interimpurity correlations present in the system. This is due to the fact that, for fixed r_0, higher density of impurities is more correlated, causing $S(\mathbf{q})$ to be more strongly suppressed at low q. This is easy to see in the case in which $r_0 = a_0$ and n_i so high that $r_i = r_0$. In this extreme case, the charge impurity distribution would be very correlated, indeed perfectly periodic, and the resistance, neglecting other scattering sources, would be zero. For each value of r_0 and carrier density n, the maximum resistivity is found to be at

$$r_i/r_0 = \sqrt{2(1 - \pi B n r_0^2)}. \tag{5}$$

In Figs. 3(a) and 3(b), we show calculated $\sigma(n)$ using different values of the impurity correlation parameters (r_0) and $S(\mathbf{q})$ given by Eq. (2) and Monte Carlo simulations. The comparison between the two results shows that the analytic continuum correlation model is qualitatively and quantitatively reliable. It is clear that, for the same value of

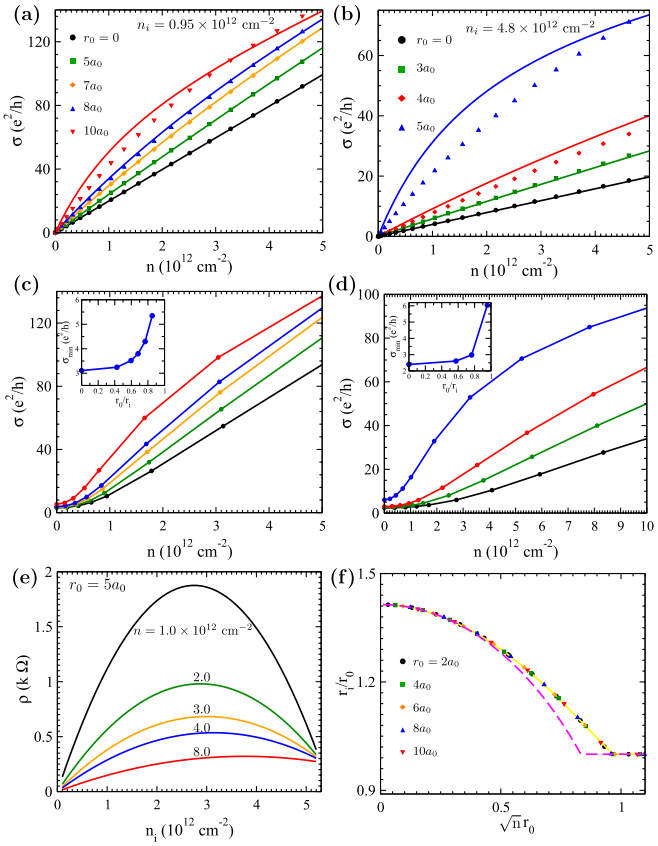

FIG. 3 (color online). Calculated $\sigma(n)$ with $S(\mathbf{q})$ obtained from the Monte Carlo simulations (symbols) and $S(\mathbf{q})$ given by Eq. (2) (solid lines) for (a) $n_i = 0.95 \times 10^{12}$ cm^{-2} and (b) $n_i = 4.8 \times 10^{12}$ cm^{-2}. (c) and (d) show the results for $\sigma(\langle n \rangle)$ obtained from the effective medium theory. The value used for n_i in (c) and (d) is the same as in (a) and (b), respectively. The insets in (c) and (d) show the value of σ_{mim} as a function of r_0/r_i. In (e), the resistivity ρ is shown as a function of impurity density n_i for different carrier densities with $r_0 = 5a_0$. (f) The relationship between r_i/r_0 and $\sqrt{n}r_0$ where the conductivity is minimum. The dashed line is obtained by using Eq. (5).

r_0, the dirtier (cleaner) system shows stronger nonlinearity (linearity) in a fixed density range consistent with experimental observation, since the larger impurity density n_i of the dirtier system allows, in principle, for stronger correlation effects to manifest themselves due to the fact that the crossover density n_c is smaller for larger n_i. To describe the transport properties close to the CNP and take into account the strong disorder-induced carrier density inhomogeneities, we use the effective medium theory [10]. Figures 3(c) and 3(d) show the effective medium theory results for $\sigma(n)$. The insets in Figs. 3(c) and 3(d) show the dependence of σ_{min} on the size of the correlation length r_0. σ_{min} increases slowly with r_0 for $r_0/r_i < 0.5$ but quite rapidly for $r_0/r_i > 0.5$. Finally, Fig. 3(e) shows that the resistivity $(1/\sigma)$ is highly nonlinear as a function of impurity density and the optimal r_i/r_0 at which the conductivity is minimum [Fig. 3(f)].

The results shown in Fig. 3 strikingly demonstrate the full power of the impurity correlation model as it clearly produces the observed experimental behavior with strong sublinear behavior for stronger impurity correlations (i.e., larger r_0). Annealing leads to stronger correlations among the impurities, since the impurities can move around to locate to equilibrium sites, thus enhancing r_0, which strongly suppress the crossover carrier density $n_c(\sim r_0^{-4})$, thus increasing the overall nonlinearity of $\sigma(n)$. In addition, the theory explains the observed strong nonlinear $\sigma(n)$ in suspended graphene [7] where the thermal or current annealing is used routinely. Finally, graphene on hexagonal BN is likely to have significant correlations in the impurity locations imposed by the similarity between graphene and BN lattice structure. This implies stronger nonlinearity in the $\sigma(n)$ dependence for a graphene-BN system as has recently been observed experimentally [17]. Although we have used a minimal model for impurity correlations, using a single correlation length parameter r_0, which captures the essential physics of correlated impurity scattering, it should be straightforward to improve the model with more sophisticated correlation models if experimental information on impurity correlations becomes available [18].

In summary, we provide a novel physically motivated explanation for the observed nonlinear behavior of graphene conductivity by showing that the inclusion of spatial correlations among the charged impurity locations leads to a significant sublinear density dependence in the conductivity in contrast to the strictly linear-in-density graphene conductivity for uncorrelated random charged impurity scattering. The great merit of our theory is that it eliminates the need for an *ad hoc* zero-range defect scattering mechanism, which has always been used in the standard model of graphene transport in order to phenomenologically explain the high-density sublinear behavior. Even though the short-range disorder is not needed to explain the sublinear behavior in our model, we do not exclude the possibility of short-range disorder scattering in real graphene samples, which would just add another resistive channel with constant conductivity. We mention that a recent experimental work [18] reports graphene transport data in remarkable agreement with the theory developed herein.

This work is supported by ONR-MURI and NRI-SWAN. E. R. acknowledges support from the Jeffress Memorial Trust, Grant No. J-1033. We thank Michael S. Fuhrer and Jun Yan for discussions and for sharing with us their unpublished experimental data. Computations were carried out in part on the SciClone Cluster at the College of William and Mary.

[1] S. Das Sarma, S. Adam, E. H. Hwang, and E. Rossi, Rev. Mod. Phys. **83**, 407 (2011).

[2] M. I. Katsnelson and A. K. Geim, Phil. Trans. R. Soc. A **366**, 195 (2008); M. I. Katsnelson, F. Guinea, and A. K. Geim, Phys. Rev. B **79**, 195426 (2009); T. O. Wehling *et al.*, Phys. Rev. Lett. **105**, 056802 (2010); F. Guinea, J. Low Temp. Phys. **153**, 359 (2008).
[3] D. K. Efetov and P. Kim, Phys. Rev. Lett. **105**, 256805 (2010); E. H. Hwang and S. Das Sarma, Phys. Rev. B **77**, 115449 (2008).
[4] K. S. Novoselov *et al.*, Proc. Natl. Acad. Sci. U.S.A. **102**, 10 451 (2005); K. S. Novoselov *et al.*, Nature (London) **438**, 197 (2005).
[5] Y.-W. Tan *et al.*, Phys. Rev. Lett. **99**, 246803 (2007).
[6] J.-H. Chen *et al.*, Nature Phys. **4**, 377 (2008).
[7] K. Bolotin *et al.*, Solid State Commun. **146**, 351 (2008); B. E. Feldman *et al.*, Nature Phys. **5**, 889 (2009).
[8] X. Hong, K. Zou, and J. Zhu, Phys. Rev. B **80**, 241415 (2009).
[9] S. Adam *et al.*, Proc. Natl. Acad. Sci. U.S.A. **104**, 18 392 (2007).
[10] E. Rossi, S. Adam, and S. Das Sarma, Phys. Rev. B **79**, 245423 (2009).
[11] E. H. Hwang, S. Adam, and S. Das Sarma, Phys. Rev. Lett. **98**, 186806 (2007).
[12] T. Ando, J. Phys. Soc. Jpn. **75**, 074716 (2006); K. Nomura and A. H. MacDonald, Phys. Rev. Lett. **98**, 076602 (2007).
[13] L. A. Ponomarenko *et al.*, Phys. Rev. Lett. **102**, 206603 (2009); F. Schedin *et al.*, Nature Mater. **6**, 652 (2007).
[14] M. Caragiu *et al.*, J. Phys. Condens. Matter **17**, R995 (2005).
[15] E. H. Hwang and S. Das Sarma, Phys. Rev. B **75**, 205418 (2007).
[16] E. Rossi and S. Das Sarma, Phys. Rev. Lett. **101**, 166803 (2008).
[17] C. R. Dean *et al.*, Nature Nanotech. **5**, 722 (2010); S. Das Sarma and E. H. Hwang, Phys. Rev. B **83**, 121405 (2011).
[18] J. Yan and M. S. Fuhrer, arXiv:1106.4835.